Author Manuscript
Author Manuscript
Author Manuscript
Author Manuscript

HHS Public Access
Author manuscript
Opt Commun. Author manuscript; available in PMC 2019 March 15.

Published in final edited form as:
Opt Commun. 2018 March 15; 411: 53–58. doi:10.1016/j.optcom.2017.10.070.

Patterned Synthesis of ZnO Nanorod Arrays for Nanoplasmonic Waveguide Applications

Thomas L. Lamson[a], **Sahar Khan**[a], **Zhifei Wang**[b], **Yun-Kai Zhang**[c], **Yong Yu**[b], **Zhe-Sheng Chen**[c], and **Huizhong Xu**[a,d,*]

[a]Department of Physics, St. John's University, Jamaica, NY 11439, USA

[b]Department of Biological Sciences, St. John's University, Jamaica, NY 11439, USA

[c]Department of Pharmaceutical Sciences, St. John's University, Jamaica, NY 11439, USA

[d]Department of Physics and Astronomy, San Francisco State University, San Francisco, CA 94132, USA

Abstract

We report the patterned synthesis of ZnO nanorod arrays of diameters between 50 nm and 130 nm and various spacings. This was achieved by patterning hole arrays in a polymethyl methacrylate layer with electron beam lithography, followed by chemical synthesis of ZnO nanorods in the patterned holes using the hydrothermal method. The fabrication of ZnO nanorod waveguide arrays is also demonstrated by embedding the nanorods in a silver film using the electroplating process. Optical transmission measurement through the nanorod waveguide arrays is performed and strong resonant transmission of visible light is observed. We have found the resonance shifts to a longer wavelength with increasing nanorod diameter. Furthermore, the resonance wavelength is independent of the nanowaveguide array period, indicating the observed resonant transmission is the effect of a single ZnO nanorod waveguide. These nanorod waveguides may be used in single-molecule imaging and sensing as a result of the nanoscopic profile of the light transmitted through the nanorods and the controlled locations of these nanoscale light sources.

Keywords

ZnO Nanorod; Nanowire Waveguide; Resonant Transmission; Surface Plasmon Polaritons

1. Introduction

The study of photonic nanowires has attracted great attention in the recent years due to their unique optical properties [1–5] and their potential in a variety of optoelectronic applications [6–17]. Among them, nanowire-based waveguide devices offer promising routes for

*Corresponding author. Address: Department of Physics & Astronomy, San Francisco State University, 1600 Holloway Avenue, San Francisco, CA 94132, USA. Tel.: +1-415-3381602; Fax: +1-415-3382178; huizhong@sfsu.edu.

Publisher's Disclaimer: This is a PDF file of an unedited manuscript that has been accepted for publication. As a service to our customers we are providing this early version of the manuscript. The manuscript will undergo copyediting, typesetting, and review of the resulting proof before it is published in its final citable form. Please note that during the production process errors may be discovered which could affect the content, and all legal disclaimers that apply to the journal pertain.

Author Manuscript Author Manuscript Author Manuscript Author Manuscript

achieving subwavelength confinement and low-loss propagation at the same time [8,9,13–15]. Dielectric materials of high refractive index were also proposed as the core of a waveguide to obtain effective subwavelength guiding [18–23], and efficient guiding of visible light through ZnO nanowire waveguides in a silver film was demonstrated [24]. These nanowire waveguides are fabricated using randomly distributed ZnO nanowires synthesized via the hydrothermal method on a glass substrate pre-seeded with ZnO nanoparticles [25]. Since ZnO nanoparticle seeds were formed by a random nucleation process during the pre-seeding step of the hydrothermal method [26–29], it is not possible to control the locations of synthesized nanowires.

On the other hand, it is highly desirable to have nanowires with controllable locations for the subsequent fabrication and application of nanowire based waveguide devices. This may be achieved with patterned fabrication of nanowire arrays where the locations of nanowires can be controlled using a top-down approach. With ZnO nanowire arrays it will also be possible to study whether transmission through ZnO nanowire waveguide arrays is affected by the array period. Such study is of particular interest since the discovery of extraordinary transmission through subwavelength aperture arrays [30]. Although ZnO nanowire arrays with controlled locations have been fabricated using a patterned growth method [31–33], the large wire sizes or dot areas make them not suitable for nanoscale light-guiding applications where individually isolated nanorods are desired.

In this work, we demonstrate the patterned synthesis of arrays of individually isolated ZnO nanorods with diameters between 50 nm and 130 nm and various spacings. ZnO nanorod waveguides were subsequently fabricated by embedding the nanorod arrays in a silver film, and optical transmission measurement through these nanorod waveguide arrays was then performed. We observed strong resonant transmission of visible light through these nanowaveguides with sizes as small as one-tenth of the incident wavelength, making them attractive devices in nanoscale light-guiding applications.

2. Method and Experiments

Electron beam lithography (EBL) is used to pattern hole arrays in a polymethyl methacrylate (PMMA) layer. ZnO nanorods in these patterned holes are subsequently synthesized using the hydrothermal method and are then embedded inside a silver metal film to form ZnO nanorod waveguides. The optical properties of these waveguides are then characterized by measuring the transmission spectrum on an inverted microscope.

The process of fabricating ZnO nanorod arrays is schematically shown in Fig. 1. First, a glass coverslip coated with a 10-nm-thick gold film is pre-seeded with ZnO nanoparticles following a recipe reported by Greene and coworkers [27]. Next, the substrate is coated with a 100-nm-thick PMMA layer and electron beam lithography is used to pattern holes in the polymer layer. Finally, ZnO nanorods are synthesized in these patterned holes using the hydrothermal method, and the PMMA layer is subsequently removed.

For the seeding process, 1 mM zinc acetate is prepared in ethanol, and 5 μL of this solution are placed drop-wise onto the gold-coated glass substrate. Upon drying, the sample is

Author Manuscript Author Manuscript Author Manuscript Author Manuscript

washed in ethanol and blown dry with nitrogen gas. After repeating this droplet process for five times, the sample is baked at 350°C for 30 minutes. This entire process is conducted three times in total.

Next, a 100-nm-thick PMMA layer is spun onto the substrate, and arrays of holes are patterned into the polymer layer using the JBX6300-FS EBL system at the Brookhaven National Laboratory. Following the exposure, the polymer was developed in 1:3 MIBK:IPA at a temperature of −25 °C for 50 seconds. The hole diameter and spacing between two neighboring holes are fixed for each array whose dimension is 400×400 μm^2. Arrays of holes with diameters ranging from 50 nm to 130 nm and spacings varying from 300 nm to 1200 nm are patterned.

Then, ZnO nanorods are grown inside the patterned holes using the hydrothermal growth method. To make the precursor solution, 20 mM solutions of zinc nitrate and hexamethylenetetramine (HMTA) are prepared separately, and 200 mL portions of the two solutions are then mixed inside a 500 mL bottle. The pre-seeded substrate is completely submerged in this solution and heated to 95°C for 70 minutes with the bottle capped. Once the sample is taken out and cooled to room temperature, it is washed in deionized water to remove any residue from the growth process, and blown dry with nitrogen gas.

The removal of the PMMA layer is conducted by washing the sample in an acetone bath for three minutes, and rinsing it with ample amount of acetone, and then blown dry with nitrogen gas. After this, the sample is baked at 350°C to remove any PMMA residues.

After removal of the polymer layer, a 100-nm-thick silver film is then deposited on the substrate using the electroplating method to form ZnO nanorod waveguides. A coating thickness of 100 nm is chosen so that direct transmission through the silver film is much smaller than the transmission of light through the ZnO nanorod waveguides. To obtain this thickness precisely, we first determine an area of the sample that will be submerged in the non-cyanide electroplating solution of silver ions (TechniSol Ag D-2460 RTU, Technic, Inc.). The current density is set to be 1 mA/cm^2 by adjusting the output of a constant current source to achieve a deposition rate of 1 nm/s. A silver plate (Alfa Aesar, 012127.FI, 99.9985%) is placed in the electroplating solution parallel to the sample such that the submerged area of the silver plate is about four times the area of the submerged portion of the sample. The sample is then electroplated for 100 s to obtain a silver film of 100 nm in thickness.

The optical properties of the ZnO nanorod waveguide arrays are examined by measuring the transmission spectrum on an Olympus IX71 inverted microscope. White light from a halogen lamp is incident onto the sample from the silver film side, and the transmitted light is collected from the glass side. The spectrum of the transmitted light is recorded for each area of interest using an Ocean Optics QE65000 spectrometer. Transmission spectrum through the gold film only is also recorded as a reference to calculate the transmission through the nanorod waveguides.

Author Manuscript Author Manuscript Author Manuscript Author Manuscript

3. Results and Discussion

After the synthesis is completed, the morphology and dimensions of the nanorods are examined using scanning electron microscopy (SEM). Some typical SEM images of the samples are shown in Figs. 2 to 4. From Fig. 2a, ZnO nanorods grow from each hole, demonstrating that our patterned synthesis approach works in producing vertically aligned ZnO nanorod arrays of controlled diameter and spacing.

By controlling the hole size, we are able to produce ZnO nanorods of diameters ranging from 50 nm to 130 nm as shown in Fig. 3. We find the morphology of the vertically aligned ZnO nanorods changes with the nanorod diameter. As shown in Figs 3a and 3b, for nanorods with diameters below 80 nm, a single nanorod grows from each hole and usually consists of two parts: a bottom part which is confined inside the hole, and a top part which expands as it grows outside the hole. For holes greater than 80 nm, we found that a bundle of ZnO nanorods with diameters between 40 and 50 nm grow out of each hole, and the overall size of the bundles does not expand much as it comes out of the hole. We have also tried holes of even larger sizes, and find that nanorods become more and more individualized with increasing hole size.

We have also fabricated nanorod arrays of different spacings ranging from 300 nm to 1200 nm, and find the morphology of the nanorods can also be affected by the spacing. As shown in Fig. 4, compared to arrays of smaller spacings, nanorods in arrays of larger spacings can grow longer and larger once they come out of holes. This is probably due to the competitive process of obtaining sufficient ions for further growth during the hydrothermal process [25].

To form the ZnO nanorod waveguides, a 100-nm-thick silver film is deposited on the substrate using the electroplating method as described in Section 2. Some SEM images of the resulting nanorod waveguides are shown in Fig. 5. Compared with Fig. 3, it is clear that the lower parts of the ZnO nanorods are now completely embedded inside the silver film while the upper parts stand above the silver film (Figs 5b–5d), creating ZnO nanowaveguides of sizes determined by the lower parts of nanorods. We also note that although the silver film is made of granular structures of sizes varying from a few nm to tens of nm, the structures are so densely packed that no pinholes are observed in the film.

Optical transmission measurements through the nanorod waveguide arrays are then performed and the results are shown in Fig. 6. We have observed a strong resonance in the transmission spectrum, which shifts to a longer wavelength with increasing nanorod diameter. In addition, the transmission at the resonance increases as the diameter of the nanorod increases.

We also find that the resonance is independent of the array period. Shown in Fig. 7a are two transmission spectra for waveguide arrays of similar diameters (95 nm) but different periods (400 nm and 800 nm). The difference in the transmission amplitude is due to the coverage ratio, which is defined as the ratio of the area covered by nanorods to the total area. By taking into account the coverage ratio, we have calculated the normalized transmission by dividing the raw transmission by the coverage ratio. The results are shown in Fig. 7b. It can be seen that the resonance wavelengths for the two spectra are about the same, and the

Author Manuscript Author Manuscript Author Manuscript Author Manuscript

transmission amplitudes at the resonance for the two spectra are comparable. We note the normalized transmission is more than 5% at the resonance wavelength of 560 nm for a nanorod waveguide array with an average diameter of about 95 nm. This level of transmission is considerably greater than that expected from an air waveguide of similar size.

The above behavior is also observed for nanorod waveguide arrays at other diameters. Using finite element method, we have conducted simulations of nanowaveguide arrays of different periods and find the resonance wavelength indeed does not change with the array period, but the transmission amplitude at the resonance can be modulated by the array period. These results strongly indicate that the observed strong resonant transmission is the effect of a single ZnO nanorod waveguide. It was known that a propagating mode can in principle exist inside a waveguide of arbitrarily small size when the dielectric constants of the cladding metal and the dielectric core are matched [21]. The dielectric constants of ZnO and silver are reasonably matched for wavelengths around 500 nm, and analysis of the modes in a single isolated ZnO waveguide of 40 nm in diameter in a silver film has shown that the fundamental mode is of plasmonic nature [22]. The imaginary part of the effective refractive index of this mode starts to increase appreciably and exceed the real part only when the wavelength is greater than 470 nm, which is more than ten times greater than the waveguide diameter. In addition to the large cutoff wavelength for these ZnO nanorod waveguides, it has been found the resonant excitation of localized surface plasmon polaritons at the entrance of the waveguide also contributes to this resonant transmission phenomenon [24].

4. Conclusion

We have fabricated arrays of vertically aligned zinc oxide nanorods with controlled diameters and spacings by combining electron beam lithography with the hydrothermal chemical synthesis method. Transmission of light through ZnO nanorod waveguides in a silver film is also studied. Strong resonant transmission of visible light through waveguides as small as one-tenth of the incident wavelength and a direct positive correlation between the resonance wavelength and the waveguide diameter are observed. We also note the resonance wavelength is independent of the array period, strongly indicating the resonant transmission phenomenon is the effect of a single ZnO nanorod waveguide. As a result of the nanoscopic profile of the transmitted light and their controlled locations, such nanorod waveguides may be used to develop new imaging and sensing techniques for applications where single-particle study of highly concentrated molecules is demanded [34].

Acknowledgments

We would like to thank Dr. Ming Lu and Dr. Aaron Stein of Brookhaven National Laboratory for many helpful discussions, and Dr. Clive Hayzelden of San Francisco State University for technical assistance with SEM imaging of the nanorod waveguides in a silver film. This research was supported by the National Science Foundation under Award No. CBET-0953645 and the National Institute of General Medical Sciences of the National Institutes of Health under Award No. R15GM116043. Research carried out in part at the Center for Functional Nanomaterials, Brookhaven National Laboratory, was supported by the U.S. Department of Energy, Office of Basic Energy Sciences, under Contract No. DEAC02-98CH10886.

Author Manuscript Author Manuscript Author Manuscript Author Manuscript

References

1. Liber CM, Wang ZL. Functional nanowires. MRS Bull. 2007; 32:99–104.
2. Yan R, Gargas D, Yang P. Nanowire photonics. Nat Photonics. 2009; 3:569–576.
3. Lal S, Hafner JH, Halas NJ, Link S, Nordlander P. Noble metal nanowires: From plasmon waveguides to passive and active devices. Acc Chem Res. 2012; 45:1887–1895. [PubMed: 23102053]
4. Wei H, Xu H. Nanowire-based plasmonic waveguides and devices for integrated nanophotonic circuits. Nanophotonics. 2012; 1:155–169.
5. Guo X, Ying Y, Tong L. Photonic nanowires: From subwavelength waveguides to optical sensors. Acc Chem Res. 2014; 47:656–666. [PubMed: 24377258]
6. Yang P, Yan H, Mao S, Russo R, Johnson J, Saykally R, Morris N, Pham J, He R, Choi HJ. Controlled growth of ZnO nanowires and their optical properties. Adv Funct Mater. 2002; 12:323–331.
7. Duan X, Huang Y, Agarwal R, Lieber CM. Single-nanowire electrically driven lasers. Nature. 2003; 421:241–245. [PubMed: 12529637]
8. Tong L, Gattass RR, Ashcom JB, He S, Lou J, Shen M, Maxwell I, Mazur E. Subwavelength-diameter silica wires for low-loss optical wave guiding. Nature. 2003; 426:816–819. [PubMed: 14685232]
9. Law M, Sirbuly DJ, Johnson JC, Goldberger J, Saykally RJ, Yang P. Nanoribbon waveguides for subwavelength photonics integration. Science. 2004; 305:1269–1273. [PubMed: 15333835]
10. Law M, Greene LE, Johnson JC, Saykally R, Yang P. Nanowire dye-sensitized solar cells. Nat Mater. 2005; 4:455–459. [PubMed: 15895100]
11. Patolsky F, Zheng G, Lieber CM. Nanowire-based biosensors. Anal Chem. 2006; 78:4260–4269. [PubMed: 16856252]
12. Sun XW, Huang JZ, Wang JX, Xu Z. A ZnO nanorod inorganic/organic heterostructure light-emitting diode emitting at 342 nm. Nano Lett. 2008; 8:1219–1223. [PubMed: 18348540]
13. Oulton RF, Sorger VJ, Genov DA, Pile DFP, Zhang X. A hybrid plasmonic waveguide for subwavelength confinement and long-range propagation. Nat Photonics. 2008; 2:496–500.
14. Oulton RF, Sorger VJ, Zentgraf T, Ma RM, Gladden C, Dai L, Bartal G, Zhang X. Plasmon lasers at deep subwavelength scale. Nature. 2009; 461:629–632. [PubMed: 19718019]
15. Guo X, Qiu M, Bao J, Wiley BJ, Yang Q, Zhang X, Ma Y, Yu H, Tong L. Direct coupling of plasmonic and photonic nanowires for hybrid nanophotonic components and circuits. Nano Lett. 2009; 9:4515–4519. [PubMed: 19995088]
16. Fang Y, Wei H, Hao F, Nordlander P, Xu H. Remote-excitation surface-enhanced Raman scattering using propagating Ag nanowire plasmons. Nano Lett. 2009; 5:2049–2053.
17. Wu X, Xiao Y, Meng C, Zhang X, Yu S, Wang Y, Yang C, Guo X, Ning CZ, Tong L. Hybrid photon-plasmon nanowire lasers. Nano Lett. 2013; 13:5654–5659. [PubMed: 24144390]
18. García de Abajo FJ. Light transmission through a single cylindrical hole in a metallic film. Opt Express. 2002; 10:1475–1484. [PubMed: 19461681]
19. Olkkonen J, Kataja K, Howe DG. Light transmission through a high index dielectric-filled sub-wavelength hole in a metal film. Opt Express. 2005; 13:6980–6989. [PubMed: 19498719]
20. Shin H, Catrysse PB, Fan S. Effect of the plasmonic dispersion relation on the transmission properties of subwavelength cylindrical holes. Phys Rev B. 2005; 72:085436.
21. Xu H, Zhu P, Craighead HG, Webb WW. Resonantly enhanced transmission of light through subwavelength apertures with dielectric filling. Opt Commun. 2009; 282:1467–1471.
22. Velasco MG, Cassidy P, Xu H. Extraordinary transmission of evanescent modes through a dielectric-filled nanowaveguide. Opt Commun. 2011; 284:4805–4809.
23. Ladanov M, Cheemalapati S, Pyayt A. Optimization of light delivery by a nanowire based single cell optical endoscope. Opt Express. 2013; 21:28001–28009. [PubMed: 24514313]
24. Garcia VL, Velasco MGM, Mamer SB, Singh KR, Hossain NK, He G, Sadoqi M, Xu H. Resonant transmission of light through ZnO nanowaveguides in a silver film. Appl Phys Lett. 2012; 101:081113.

Author Manuscript Author Manuscript Author Manuscript Author Manuscript

25. Lopez OE, Tucker AL, Singh KR, Mamer SB, Sadoqi M, Xu H. Synthesis of zinc oxide nanowires on seeded and unseeded gold substrates: Role of seed nucleation and precursor concentration. Superlattices Microstruct. 2014; 75:358–370.
26. Vayssieres L. Growth of arrayed nanorods and nanowires of ZnO from aqueous solutions. Adv Mater. 2003; 15:464–466.
27. Greene LE, Law M, Goldberger J, Kim F, Johnson JC, Zhang Y, Saykally RJ, Yang P. Low-temperature wafer-scale production of ZnO nanowire arrays. Angew Chem Int Ed. 2003; 42:3031–3034.
28. Greene LE, Law M, Tan DH, Montano M, Goldberger J, Somorjai G, Yang P. General route to vertical ZnO nanowire arrays using textured ZnO seeds. Nano Lett. 2005; 5:1231–1236. [PubMed: 16178216]
29. Baruah S, Dutta J. Hydrothermal growth of ZnO nanostructures. Sci Technol Adv Mater. 2009; 10:013001. [PubMed: 27877250]
30. Ebbesen TW, Lezec HJ, Ghaemi HF, Thio T, Wolff PA. Extraordinary optical transmission through sub-wavelength hole arrays. Nature. 1998; 391:667–669.
31. Xu S, Wei Y, Kirkham M, Liu J, Mai W, Davidovic D, Snyder RL, Wang ZL. Patterned growth of vertically aligned ZnO nanowire arrays on inorganic substrates at low temperature without catalyst. J Am Chem Soc. 2008; 130:14958–14959. [PubMed: 18921981]
32. Ahsanulhaq Q, Kim JH, Kim JH, Hahn YB. Seedless pattern growth of quasi-aligned ZnO nanorod arrays on cover glass substrates in solution. Nanoscale Res Lett. 2010; 5:669–674.
33. Wang S, Song C, Cheng K, Dai S, Zhang Y, Du Z. Controllable growth of ZnO nanorod arrays with different densities and their photoelectric properties. Nanoscale Res Lett. 2012; 7:246. [PubMed: 22559262]
34. Pollack L, Webb WW. Complex molecular dynamics in the spotlight. Nat Biotechnol. 2010; 28:564–565. [PubMed: 20531335]

Author Manuscript Author Manuscript Author Manuscript Author Manuscript

Highlights

- ZnO nanorod arrays with diameters ranging from 50 nm to 130 nm are synthesized.
- Strong resonant transmission through ZnO nanorod waveguides in silver is observed.
- The resonance shifts to a longer wavelength with increasing waveguide diameter.
- The resonance wavelength is independent of the ZnO nanowaveguide array period.

Author Manuscript Author Manuscript Author Manuscript Author Manuscript

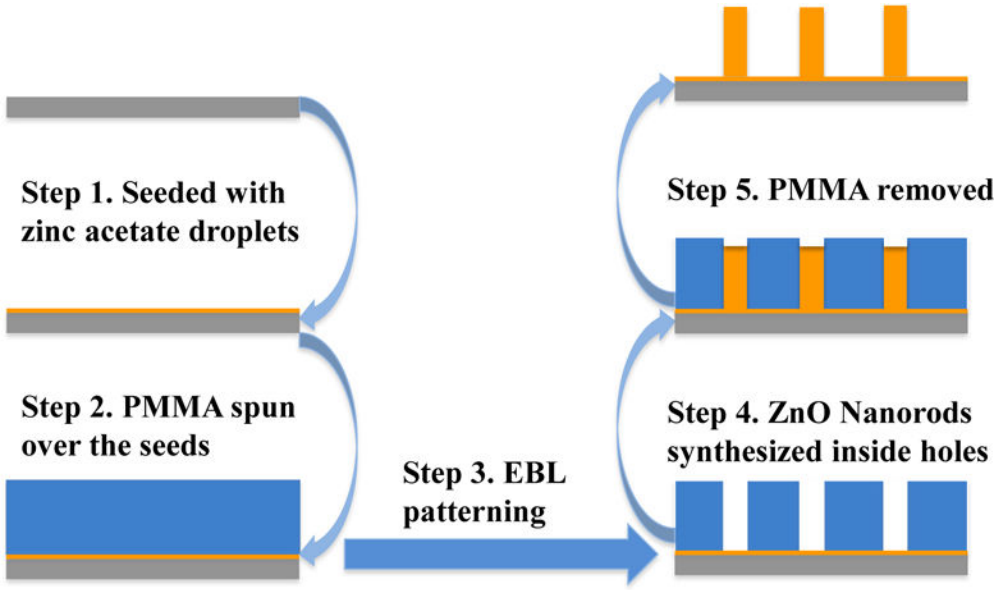

Fig. 1.

Schematics of the ZnO nanorod array fabrication process. In step 1, the substrate is seeded with droplets of zinc acetate. In step 2, a layer of PMMA is spun onto the substrate followed by patterning of holes with EBL in step 3. In step 4, vertically aligned ZnO nanorods are grown inside the holes using the hydrothermal method. The PMMA is subsequently removed in step 5.

Author Manuscript Author Manuscript Author Manuscript Author Manuscript

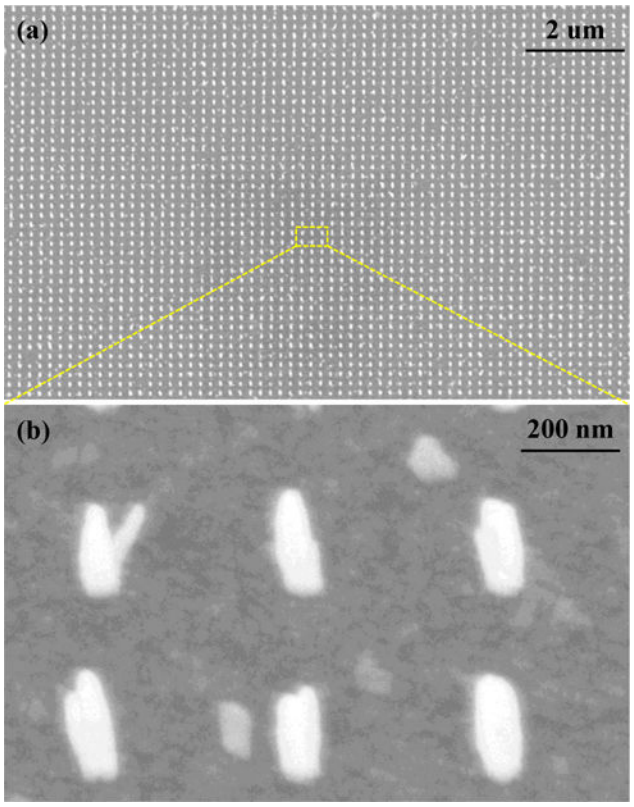

Fig. 2.

SEM images of ZnO nanorod arrays synthesized inside PMMA holes patterned with EBL. Both images are viewed with a 20° tilt angle. Image (b) is a close-up view of the box shown in image (a). The array has a period of 400 nm, and the lower parts of the nanorods have an average diameter of 75 nm.

Author Manuscript Author Manuscript Author Manuscript Author Manuscript

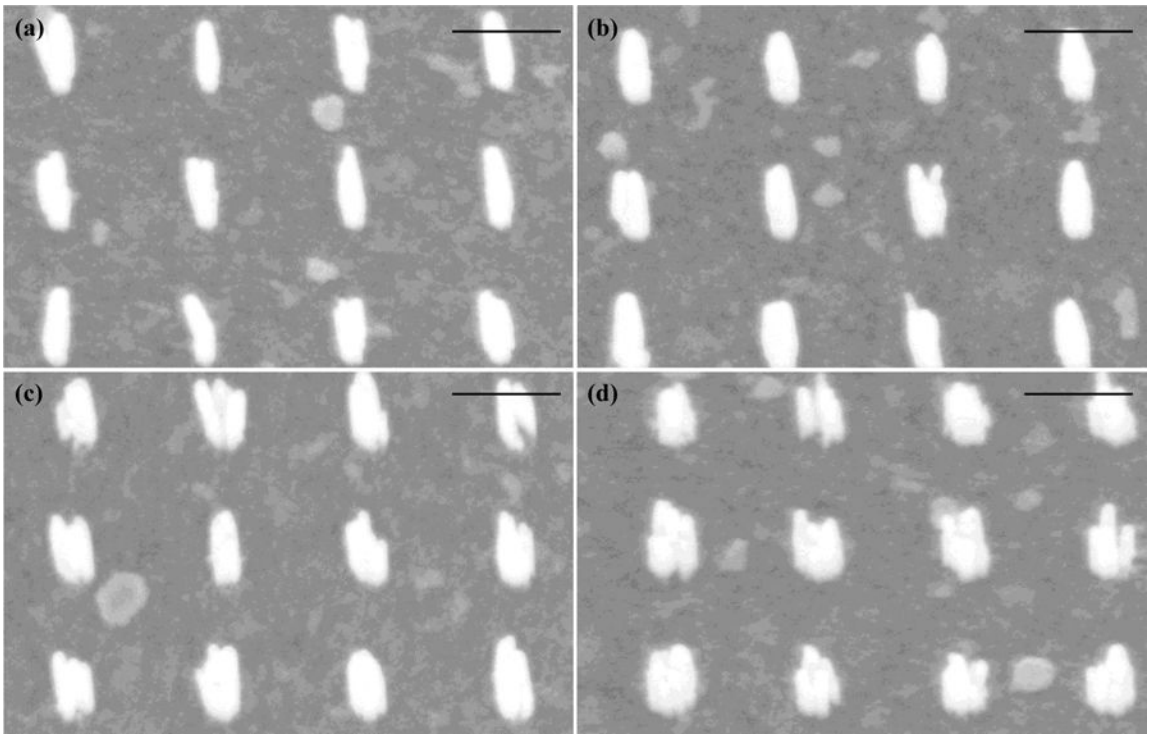

Fig. 3.

SEM images of ZnO nanorod arrays synthesized inside PMMA holes patterned with EBL. All images are viewed with a 20° tilt angle. The array has a period of 400 nm, and the lower parts of the nanorods have an average diameter of (a) 59 nm, (b) 75 nm, (c) 95 nm, and (d) 126 nm respectively. All scale bars are 300 nm.

Author Manuscript Author Manuscript Author Manuscript Author Manuscript

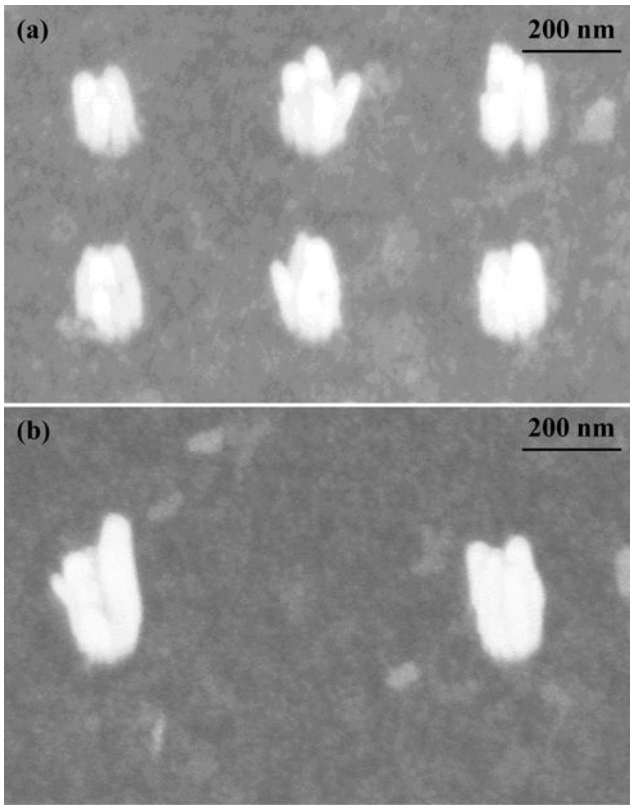

Fig. 4.

SEM images of ZnO nanorod arrays synthesized inside PMMA holes patterned with EBL. Both images are viewed with a 20° tilt angle. The array has a period of (a) 400 nm and (b) 800 nm. The lower parts of the nanorods have an average diameter of 126 nm for both samples.

Author Manuscript Author Manuscript Author Manuscript Author Manuscript

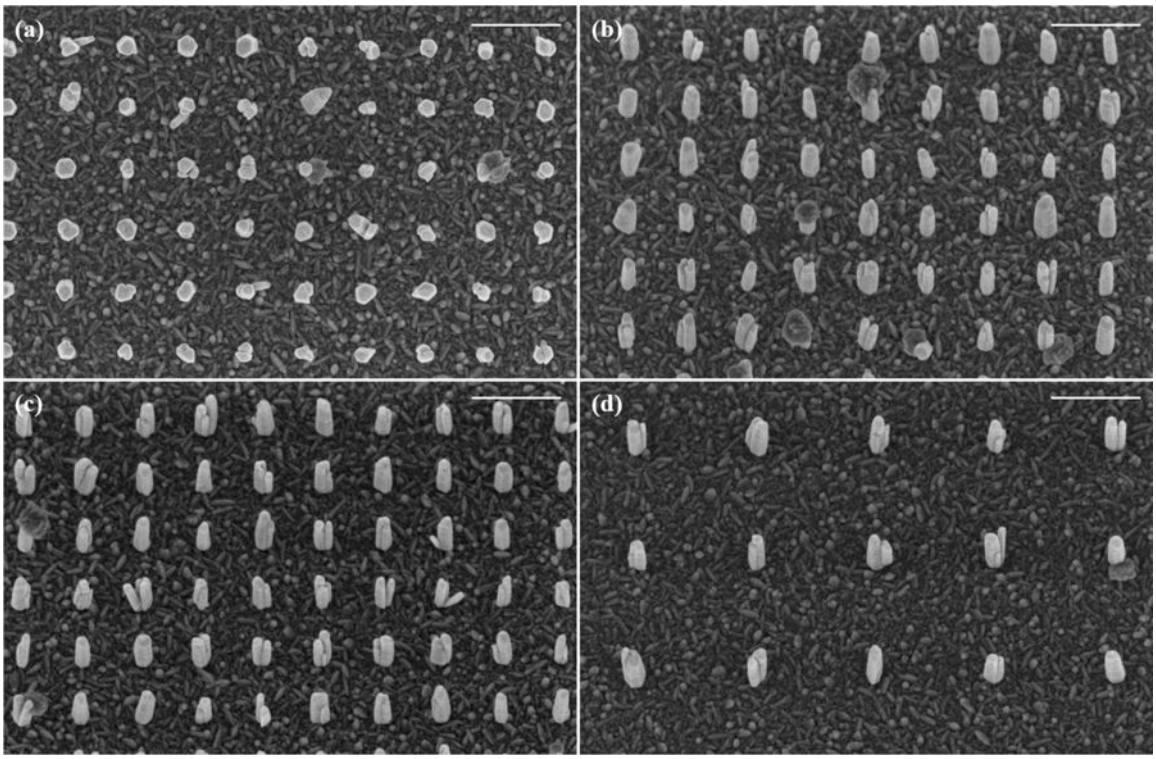

Fig. 5.

SEM images of ZnO nanorod waveguides formed by embedding the lower parts of nanorods inside a dense silver film. (a) Top view and (b) 20° tilt view of a nanorod waveguide array with a period of 400 nm and an average diameter of 59 nm for the lower parts of nanorods. 20° tilt view of nanorod arrays of similar average diameter for the lower parts of nanorods (75 nm) but two different periods: (c) 400 nm, and (d) 800 nm. All scale bars are 300 nm.

Author Manuscript Author Manuscript Author Manuscript Author Manuscript

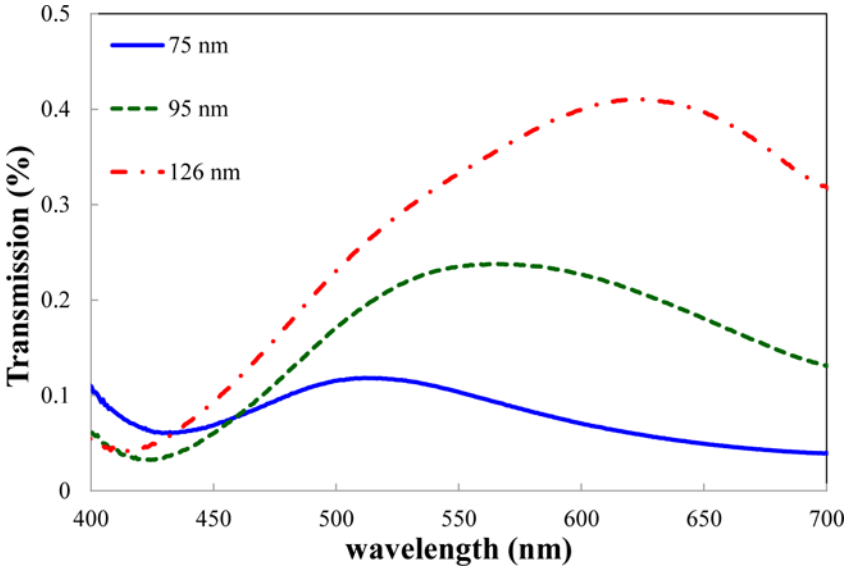

Fig. 6.

Raw transmission spectra through ZnO nanorod waveguide arrays of three different nanorod diameters: 75 nm (solid lines), 95 nm (dashed lines), and 126 nm (dash-dotted lines). The three arrays have the same period of 400 nm.

Author Manuscript Author Manuscript Author Manuscript Author Manuscript

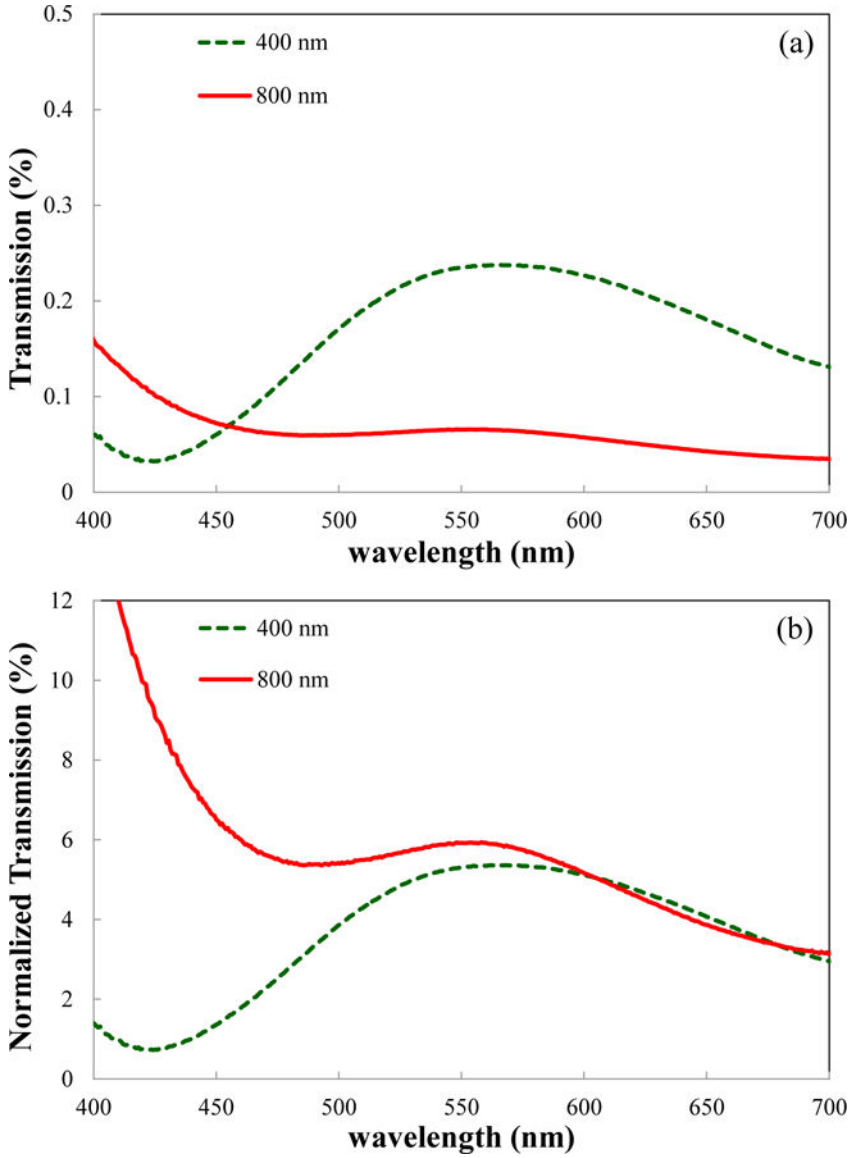

Fig. 7.

Transmission spectra through ZnO nanowaveguide arrays of similar diameters (95 nm) but different spacings: 400 nm (dashed lines) and 800 nm (solid lines). (a) Raw transmission spectra. (b) Transmission normalized by the coverage ratio.